Laser Doppler Velocimetry for Joint Measurements of Acoustic and Mean Flow Velocities: LMS-Based Algorithm and CRB Calculation

Laurent Simon, *Member, IEEE*, Olivier Richoux, Anne Degroot, and Louis Lionet

***Abstract*—This paper presents a least-mean-square (LMS) algorithm for the joint estimation of acoustic and mean flow velocities from laser Doppler velocimetry (LDV) measurements. The usual algorithms used for measuring with LDV purely acoustic velocity or mean flow velocity may not be used when the acoustic field is disturbed by a mean flow component. The LMS-based algorithm allows accurate estimations of both acoustic and mean flow velocities. The Cramér–Rao bound (CRB) of the associated problem is determined. The variance of the estimators of both acoustic and mean flow velocities is also given. Simulation results of this algorithm are compared with the CRB, and the comparison leads us to validate this estimator.**

***Index Terms*—Acoustic velocity, Cramér–Rao bound (CRB), laser Doppler velocimetry (LDV), least-mean-square (LMS) method, mean flow velocity.**

I. Introduction

THE LASER doppler velocimeter (LDV) is an optical technique allowing direct measurement of local and instantaneous fluid velocity. This method is nonintrusive and is based on optical interferometry for estimating the velocity of scatterers suspended in a fluid by means of the frequency analysis of the light scattered by the seeding particles [1].

For fluid mechanics measurements, the particle velocity can be considered as constant during the transit time of the seeding particle through the measurement volume (defined by the interferometry fringe volume), and the frequency of the LDV signal is constant during this period [2]. Typical orders of magnitude of mean flow velocities are from a few meters per second up to higher than the acoustic celerity (supersonic flow). The data processing consists then to estimate the power spectral density (PSD) of the velocity signal from Poisson-based randomly distributed samples. PSD may be estimated by interpolating the randomly distributed samples, by resampling the interpolating signal, and by compensating the effect of interpolation in the Fourier domain [3], [4]. The autocorrelation function (ACF) may also be reconstructed from the randomly distributed samples, and the Fourier transform of the estimated ACF gives an estimation of the PSD [5]. Finally, Kalman filtering may be used to estimate the PSD [6].

Manuscript received March 20, 2007; revised September 11, 2007.

The authors are with LAUM, CNRS, University of Le Mans, 72085 Le Mans, France.

Color versions of one or more of the figures in this paper are available online at http://ieeexplore.ieee.org.

Digital Object Identifier 10.1109/TIM.2008.917670

For sine acoustic excitation, the particle velocity is no longer constant, and the LDV signal is frequency modulated [7], [8]. To estimate the particle velocity from these signals, specific signal processing techniques are used, such as spectral analysis [9]–[11], photon correlation [12], or frequency demodulation associated with postprocessing methods [13]–[15]. Typical orders of magnitude of mean flow velocities are from a few micrometers per second up to 100 mm/s for frequencies from 10 to 4000 Hz.

On one hand, for most acoustic measurements, the particle velocity can be considered as the sum of an ac component due to acoustic excitation and a weak dc contribution due to flow. When the particle oscillates in the measurement volume during some acoustic periods, the effect of the flow can be reduced, and usual postprocessing methods may be used [13]–[16].

On the other hand, the dc-flow component in many cases prevents the use of the postprocessing methods given in [13]–[15] because the signal time length is less or largely less than one acoustic period. The aim of this paper is to estimate both the dc (flow) and ac (acoustic) components from such LDV signals.

Lazreq and Ville [17] measured the acoustic velocity in the presence of mean flow by means of a probe consisting of a hot wire and a microphone. Their results showed a good agreement between the theory and the experiment, but this probe cannot be considered as nonintrusive. LDV has also been used by adapting the slotting technique to estimate the acoustic particle velocity in a turbulent flow [18] with a 2-D LDV velocimeter. The acoustic impedance was estimated by means of an LDV probe and with a microphone probe, and the different results were compared. Finally, Boucheron *et al.* [19] have developed a new method of signal processing, called "perio-correlation," to estimate sine acoustic velocity in strong mean flow by LDV.

In this paper, the sine acoustic excitation is supposed to be perfectly known, and a frequency demodulation technique [15] is performed to estimate the particle velocity from the LDV signal. In this paper, we propose a new method to jointly estimate the acoustic particle velocity (amplitude and phase) and the mean flow velocity from the velocity signal. This method is based on the least-mean-square (LMS) algorithm. The mean flow velocity and the amplitude and phase of acoustic particle velocity are estimated for each seeding particle crossing the measurement volume. Furthermore, the Cramér–Rao bound (CRB) of the associated problem is calculated. The CRB gives the lowest variance of any unbiased estimator and,

0018-9456/$25.00 © 2008 IEEE

Authorized licensed use limited to: Laurent Simon. Downloaded on July 6, 2009 at 10:10 from IEEE Xplore. Restrictions apply.

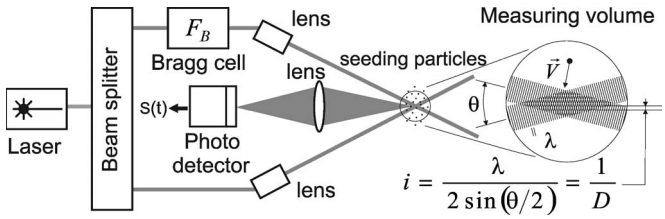

Fig. 1. Optical setup of an LDV system. When the particle q crosses the measurement volume, the light is scattered in all directions, and the burst signal $s_q(t)$ is collected by the photodetector. Data processing of $s_q(t)$ allows us then to estimate the mean flow and particle acoustic velocities.

consequently, theoretically yields the minimum uncertainties linked to the velocity estimations (acoustic and mean flow velocities). Finally, simulated data are processed to validate the LMS-based algorithm and to compare the variance of the results with the CRB.

Section II deals with the LDV principles, including the velocity signal modeling and the associated signal processing for acoustic applications. In Section III, data processing based on the LMS algorithm is explained, and the CRBs of both the mean flow and acoustic velocities are determined. Finally, the results of the Monte Carlo simulation are shown and compared to the CRBs in Section IV for acoustic frequencies from 125 to 4000 Hz, for acoustic velocities from 0.05 to 50 mm $\cdot$ s^{-1}, and for mean flow velocities from 0.05 to 5000 mm $\cdot$ s^{-1}.

II. Fundamentals of LDV

In this section, we consider time-varying signals such that $t \in [t_q - T_q/2, t_q + T_q/2]$, with t_q being the central time of the signal, T_q being a time of flight, and q associated with a given seeding particle.

A. LDV Principle

In the differential mode, two coherent laser beams are crossed and focused to generate an ellipsoidal probe volume, in which the electromagnetic interferences lead to apparent dark and bright fringes [1].

The velocity $v_q(t)$ of the seeding particle, which is denoted q, is related to the scattered optical field due to the Doppler effect. The light intensity scattered by the particle crossing the probe volume is modulated in amplitude and frequency. The frequency of modulation $F_q(t)$ is called the Doppler frequency and is given by

$$F_q(t) = \frac{v_q(t)}{i} = \frac{2v_q(t)}{\lambda_L}\sin(\theta/2) \tag{1}$$

where $v_q(t)$ is the velocity of the particle along the x-axis, and i is the fringe spacing expressed as a function of the angle θ between the incoming laser beams and their optical wavelength λ_L (Fig. 1).

The diffused light is collected by a receiving optics and is converted into an electrical signal by a photomultiplier (PM). This signal can then be modeled as [15]

$$s_q(t) = A_q(t)\left(M + \cos\,\phi_q(t)\right) \tag{2}$$

where M takes into account the positive sign of the CRB of the light intensity. In (2), the amplitude modulation linked to the normally distributed light intensity across the beam section is written as

$$A_q(t) = K_q e^{-(\beta d_q(t))^2} \tag{3}$$

where K_q is related to the laser beam, the PM sensitivity, the electronic amplification, the observation direction, and the scattering efficiency of particle q. Furthermore, β is related to the probe geometry, and $d_q(t)$ is the projection of the time-varying particle displacement along the x-axis in the probe volume. Similarly, the phase modulation in (2) is described by

$$\phi_q(t) = 2\pi\frac{d_q(t)}{i} + \phi_0 \tag{4}$$

where ϕ_0 is the initial phase due to the optical setup. Furthermore, we denote $x_q(t)$ as the signal such that

$$x_q(t) = s_q(t) + w(t) \tag{5}$$

where $w(t)$ is the additive noise [13].

To avoid any ambiguity on the sign of the velocity, a Bragg cell tuned to frequency $F_B = 40$ MHz is used to shift the frequency of one of the lasers. The signal $s_q(t)$ is consequently written as

$$s_q(t) = A_q(t)\left(M + \cos(2\pi F_B t + 2\pi d_q(t)/i + \phi_0)\right). \tag{6}$$

The offset component M is then canceled by a high-pass filtering, and the signal $s_q(t)$ is downshifted to zero thanks to a quadrature demodulation technique [20]. The actual signal, which is called burst signal, can finally be written as

$$s_q(t) = A_q(t)\cos\left(2\pi d_q(t)/i + \phi_0\right). \tag{7}$$

B. Doppler Signal Modeling in Acoustics

Considering only pure sine acoustic waves and supposing that the mean flow velocity is constant inside the probe volume, the projection along the x-axis of the velocity of a particle q jointly subjected to the sine acoustic wave and the mean flow field can be expressed as

$$v_q(t) = v_{c,q} + V_{\rm ac}\cos(2\pi F_{\rm ac}t + \phi_{\rm ac}) \tag{8}$$

where $v_{c,q}$ is the mean flow velocity of particle q, $V_{\rm ac}$ and $\phi_{\rm ac}$ are the amplitude and phase of the acoustic particle velocity, respectively, and $F_{\rm ac}$ is the known frequency of the pure sine acoustic excitation. The amplitude modulation of the burst signal (3) associated with the particle q may be written as

$$A_q(t) = K_q \exp\left[-\beta\left(v_{c,q}(t-t_q) + \frac{V_{\rm ac}}{2\pi F_{\rm ac}}\sin(2\pi F_{\rm ac}t + \phi_{\rm ac})\right)^2\right]. \tag{9}$$

Similarly, the phase modulation (4) of the burst signal associated to the particle q is

$$\phi_q(t) = \frac{2\pi}{i}v_{c,q}(t - t_q) + \frac{V_{\rm ac}}{2\pi i F_{\rm ac}}\sin(2\pi F_{\rm ac}t + \phi_{\rm ac}). \tag{10}$$

Authorized licensed use limited to: Laurent Simon. Downloaded on July 6, 2009 at 10:10 from IEEE Xplore. Restrictions apply.

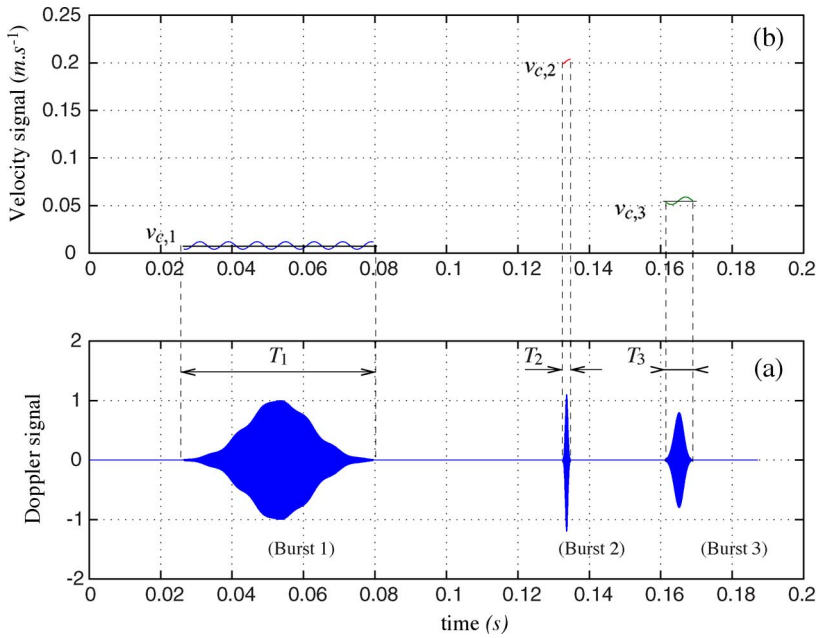

Fig. 2. (a) Example of a Doppler signal. (b) Associated velocity signal. Burst 1 is associated with a low mean flow velocity corresponding to $N_{\rm per}$ acoustic periods largely higher than 1. Burst 2 is associated with a high mean flow velocity corresponding to $N_{\rm per}$ acoustic period largely lower than 1. Burst 3 is associated with a mean flow velocity corresponding to $N_{\rm per} \lesssim 1$ acoustic period.

We note that the flow velocity $v_{c,q}$ can change from one particle q to another, whereas the acoustic parameters $V_{\rm ac}$ and $\phi_{\rm ac}$ are independent of q. Thus, when the acoustic wave is disturbed by a mean flow, assuming that the particles q cross the measurement volume at different random central times t_q, without time overlapping between bursts q and $q+1$, the Doppler signal can be written as

$$s(t) = \sum_q s_q(t) = A_D(t)\cos\left[\phi_D(t)\right] \tag{11}$$

where the amplitude and phase, respectively, are expressed as

$$A_D(t) = \begin{cases} A_q(t), & t \in [t_q - T_q/2, t_q + T_q/2] \\ 0, & \text{otherwise} \end{cases} \tag{12}$$

$$\phi_D(t) = \begin{cases} \phi_q(t), & t \in [t_q - T_q/2, t_q + T_q/2] \\ 0, & \text{otherwise.} \end{cases} \tag{13}$$

Furthermore, the time of flight of the particle q is defined as [21]

$$T_q = \frac{\sqrt{2}D_x}{v_{c,q}} \tag{14}$$

where D_x is the length of the probe volume in the x-axis, and the associated number of acoustic periods is

$$N_{\rm per} = \frac{\sqrt{2}D_x}{v_{c,q}} F_{\rm ac}. \tag{15}$$

As expected, the faster the particle crosses the probe volume, the lower the time of flight and the number of acoustic periods. An example of a typical Doppler signal is shown in Fig. 2(a), where the different particle times of flight are associated with different mean flow velocities.

C. Doppler Signal Processing

The aim of the signal processing developed after sampling the Doppler signal is to estimate jointly and burst by burst the acoustic particle velocity (amplitude $V_{\rm ac}$ and phase $\phi_{\rm ac}$) and the mean flow velocity $v_{c,q}$. This procedure is usually split into two stages. First, after a detection procedure [21], a frequency demodulation of the Doppler signal $s(t)$ is performed using a time–frequency transform to estimate the instantaneous frequency $F_q(t)$ [or, equivalently, (1)] and the velocity signal $v_q(t)$, burst by burst [14]. Note that the detector only selects bursts corresponding to one tracer in the measurement volume. Second, the data processing of the estimated velocity signal $\hat{v}_q(t)$ allows us to obtain both components of the acoustic and mean flow velocities for each burst. This first stage is described in this section, whereas the second stage (data LMS-based processing) is explained in Section IV.

According to (1), the velocity signal associated with the particle q is expressed as

$$v_q(t) = iF_q(t) \tag{16}$$

where i is the fringe spacing. Thus, the problem consists of estimating the mean value $\hat{v}_{c,q}$, the amplitude $\hat{V}_{\rm ac}$, and the phase $\hat{\phi}_{\rm ac}$ of the estimated velocity signal associated with each burst q from the actual noisy burst signal $x_q(t)$. Fig. 2(a) and (b) shows an example of a noiseless simulated Doppler signal and the associated velocity signal for three nonoverlapping bursts, respectively.

In Section III, the CRB of the problem is calculated. Then, a method based on an LMS algorithm is presented in Section IV and is applied to simulated velocity signals $v_q(t)$ in Section V.

Authorized licensed use limited to: Laurent Simon. Downloaded on July 6, 2009 at 10:10 from IEEE Xplore. Restrictions apply.

III. CRB Calculation

We recall that the CRB gives the lowest bound of the variance an unbiased estimator may reach (if it exists) [22]. As explained in [22], the CRB alerts us to the physical impossibility of finding an unbiased estimator whose variance is less than the bound. In the case of single-tone signals, the CRBs were calculated by Rife and Boorstyn [23] in 1974. The CRBs of LDV signals were also studied in the case of fluid mechanics [24], [25]. In the case of sine acoustic excitation, the CRBs of LDV signals were also studied by Le Duff *et al.* [20].

We focus here on the problem of calculating the CRB of the following problem. The velocity data are assumed to be such that

$$u[n] = v[n;\theta] + w[n] \tag{17}$$

for $n \in [n_0, n_1]$, where $w[n]$ is the white Gaussian noise, $w[n] \sim \mathcal{N}(0, \sigma^2)$, the data being modeled according to

$$v[n;\theta] = v_c + V_{\rm ac}\cos(2\pi f_{\rm ac} n + \phi_{\rm ac}) \tag{18}$$

where $f_{\rm ac} = F_{\rm ac}/F_s$, F_s being the sampling frequency, $v_c \equiv v_{c,q}$, and where the unknown parameters are gathered in

$$\theta = [\, v_c \quad V_{\rm ac} \quad \phi_{\rm ac}\,]^T. \tag{19}$$

We furthermore suppose that $f_{\rm ac} \neq 0$ and that $f_{\rm ac} \neq 1/2$.

A. CRB for One Burst

The CRB is given by the inverse of the Fisher information matrix $\mathbf{J}(\theta)$, $\mathrm{CRB}(\theta) = \mathbf{J}(\theta)^{-1}$, where the Fisher information matrix is given by [22]

$$\mathbf{J}(\theta)_{kl} = \frac{1}{\sigma^2}\sum_{n=n_0}^{n_1} \frac{\partial v[n;\theta]}{\partial \theta_k}\frac{\partial v[n;\theta]}{\partial \theta_l} \tag{20}$$

for $k, l \in [1, 3]$, for $\theta = [\, v_c \quad V_{\rm ac} \quad \phi_{\rm ac}\,]^T$. The derivatives in (20), according to (18), lead to (21), shown at the bottom of the page, where $N = n_1 - n_0 + 1$, and where

$$\gamma = \pi f_{\rm ac} \tag{22}$$

$$\beta = 2\pi f_{\rm ac} n_0 + \pi f_{\rm ac}(N-1) + \phi_{\rm ac}. \tag{23}$$

We define the linear signal-to-noise ratio (SNR) of the velocity signal as

$$\mathrm{SNR} = \frac{V_{\rm ac}^2}{2\sigma^2} \tag{24}$$

and we then have, upon inversion, (25)–(27), shown at the bottom of the page.

B. CRB for N_b Bursts

We now assume that the algorithm developed in Section III-A is used to estimate the unknown parameters $\theta = [\, v_c \quad V_{\rm ac} \quad \phi_{\rm ac}\,]^T$, in the case of N_b bursts. The main difference between this problem and the problem developed above is that the index n_0 is no longer a constant but might be modeled as a discrete random variable, uniformly distributed in $[0, n_{\rm ac}]$, where $N_{\rm ac} = \mathrm{nint}[F_s/F_{\rm ac}]$, nint[] being the nearest integer. As a consequence, the discrete random variable β given in (23), which appears in (26) and (27), is uniformly distributed in $[\pi(N-1)f_{\rm ac} + \phi_{\rm ac}, \pi(N-1)f_{\rm ac} + \phi_{\rm ac} + 2\pi]$. Averaging the terms linked to β in (26) and (27) consequently leads to

$$\langle \cos(2\beta)\rangle = \langle \sin(2\beta)\rangle = 0 \tag{28}$$

$$\langle \cos^2(\beta)\rangle = \langle \sin^2(\beta)\rangle = \frac{1}{2}. \tag{29}$$

$$\mathbf{J}(\theta) = \frac{1}{\sigma^2}\begin{pmatrix} N & \frac{\cos(\beta)\sin(\gamma N)}{\sin(\gamma)} & -\frac{V_{\rm ac}\sin(\beta)\sin(\gamma N)}{\sin(\gamma)} \\ \frac{\cos(\beta)\sin(\gamma N)}{\sin(\gamma)} & \frac{N}{2} + \frac{\cos(2\beta)\sin(2\gamma N)}{2\sin(2\gamma)} & -\frac{V_{\rm ac}\sin(2\beta)\sin(2\gamma N)}{2\sin(2\gamma)} \\ -\frac{V_{\rm ac}\sin(\beta)\sin(\gamma N)}{\sin(\gamma)} & -\frac{V_{\rm ac}\sin(2\beta)\sin(2\gamma N)}{2\sin(2\gamma)} & \frac{NV_{\rm ac}^2}{2} - \frac{V_{\rm ac}^2\cos(2\beta)\sin(2\gamma N)}{2\sin(2\gamma)} \end{pmatrix} \tag{21}$$

$$\mathrm{var}(v_c) \geq \mathrm{CRB}(v_c) = \frac{V_{\rm ac}^2}{4\mathrm{SNR}}\frac{N^2 - \left(\frac{\sin(2\gamma N)}{\sin(2\gamma)}\right)^2}{\frac{N^3}{2} - \frac{N}{2}\left(\frac{\sin(2\gamma N)}{\sin(2\gamma)}\right)^2 - N\left(\frac{\sin(\gamma N)}{\sin(\gamma)}\right)^2 + \frac{\sin(2\gamma N)}{\sin(2\gamma)}\left(\frac{\sin(\gamma N)}{\sin(\gamma)}\right)^2} \tag{25}$$

$$\mathrm{var}(V_{\rm ac}) \geq \mathrm{CRB}(V_{\rm ac}) = \frac{V_{\rm ac}^2}{2\mathrm{SNR}}\frac{N^2 - N\,\cos(2\beta)\frac{\sin(2\gamma N)}{\sin(2\gamma)} - 2\,\sin^2(\beta)\left(\frac{\sin(\gamma N)}{\sin(\gamma)}\right)^2}{\frac{N^3}{2} - \frac{N}{2}\left(\frac{\sin(2\gamma N)}{\sin(2\gamma)}\right)^2 - N\left(\frac{\sin(\gamma N)}{\sin(\gamma)}\right)^2 + \frac{\sin(2\gamma N)}{\sin(2\gamma)}\left(\frac{\sin(\gamma N)}{\sin(\gamma)}\right)^2} \tag{26}$$

$$\mathrm{var}(\phi_{\rm ac}) \geq \mathrm{CRB}(\phi_{\rm ac}) = \frac{1}{2\mathrm{SNR}}\frac{N^2 + N\,\cos(2\beta)\frac{\sin(2\gamma N)}{\sin(2\gamma)} - 2\,\cos^2(\beta)\left(\frac{\sin(\gamma N)}{\sin(\gamma)}\right)^2}{\frac{N^3}{2} - \frac{N}{2}\left(\frac{\sin(2\gamma N)}{\sin(2\gamma)}\right)^2 - N\left(\frac{\sin(\gamma N)}{\sin(\gamma)}\right)^2 + \frac{\sin(2\gamma N)}{\sin(2\gamma)}\left(\frac{\sin(\gamma N)}{\sin(\gamma)}\right)^2} \tag{27}$$

Authorized licensed use limited to: Laurent Simon. Downloaded on July 6, 2009 at 10:10 from IEEE Xplore. Restrictions apply.

This finally yields (30) and (31), shown at the bottom of the page.

In the following, we use (25) for v_c and (30) for $V_{\rm ac}$ to study the CRB of the problem. We recall that N depends on v_c (36). As a consequence, the CRBs of v_c (25) and $V_{\rm ac}$ (30) both depend on v_c and $V_{\rm ac}$, whereas the CRB of $\phi_{\rm ac}$ (31) is independent of $V_{\rm ac}$.

C. Asymptotic Behavior of the CRB

In Appendix A, we give the expressions of the asymptotic CRB of θ, for both cases $2\gamma N \ll 1$ $(N_{\rm per} \ll 1/(2\pi))$ and $2\gamma N \gg 1$ $(N_{\rm per} \gg 1/(2\pi))$.

In the asymptotic case $2\gamma N \ll 1$, we prove [see (63) and (64)] that the relative variances of v_c and $V_{\rm ac}$ are

$$\frac{\mathrm{var}(v_c)}{v_c^2} \geq \frac{\mathrm{CRB}(v_c)}{v_c^2} = \frac{1}{\mathrm{SNR}} \frac{45}{\pi^4 2^{7/2}} \frac{1}{D_x^5 F_s} \frac{v_c^3 V_{\rm ac}^2}{F_{\rm ac}^4} \tag{32}$$

$$\frac{\mathrm{var}(V_{\rm ac})}{V_{\rm ac}^2} \geq \frac{\mathrm{CRB}(V_{\rm ac})}{V_{\rm ac}^2} = \frac{1}{\mathrm{SNR}} \frac{45}{\pi^4 2^{9/2}} \frac{1}{D_x^5 F_s} \frac{v_c^5}{F_{\rm ac}^4}. \tag{33}$$

Both CRBs of v_c and $V_{\rm ac}$ are proportional to $v_c^5 V_{\rm ac}^2$ and inversely proportional to $F_{\rm ac}^4$. Consequently, doubling the mean flow velocity yields a 15-dB increase of the variance of both v_c and $V_{\rm ac}$. Similarly, doubling the amplitude of the acoustic particle velocity $V_{\rm ac}$ leads to a 6-dB increase of the variance of both v_c and $V_{\rm ac}$. Finally, doubling the frequency of the pure sine acoustic wave leads to a 12-dB decrease of the variance of both v_c and $V_{\rm ac}$. We also note that doubling the length of the probe volume D_x yields a 15-dB decrease of the variance of both v_c and $V_{\rm ac}$.

In the asymptotic case $2\gamma N \gg 1$, we prove that [see (72) and (73)]

$$\mathrm{var}(v_c) \geq \frac{1}{\mathrm{SNR}} \frac{1}{2^{3/2} D_x F_s} v_c V_{\rm ac}^2 \tag{34}$$

$$\mathrm{var}(V_{\rm ac}) \geq \frac{1}{\mathrm{SNR}} \frac{1}{\sqrt{2} D_x F_s} v_c V_{\rm ac}^2. \tag{35}$$

Due to the exact [see (25), (30), and (31)] and asymptotic (32)–(35) expressions of the CRB, the minimum uncertainties linked to the velocity estimations (acoustic and mean flow velocities) are completely known. In Section IV, the LMS-based algorithm is introduced. It is then applied in Section V to simulated data to be compared with the CRB.

IV. LMS Algorithm

From a practical point of view, the actual velocity signal is uniformly sampled. Consequently, the number of samples N_q associated with the particle q is derived from (14) as

$$N_q = \frac{\sqrt{2} D_x F_s}{v_{c,q}} \tag{36}$$

and the associated number of acoustic periods (15) is now defined as

$$N_{\rm per} = \frac{\sqrt{2} D_x}{v_{c,q}} F_{\rm ac}. \tag{37}$$

The sine-wave fit is then solved by minimizing the cost function $V(\theta)$

$$V(\theta) = \frac{1}{N} \sum_{n=n_0}^{n_1} \left(u[n] - v[n;\theta]\right)^2 \tag{38}$$

with respect to the unknown parameters θ (19), where $u[n]$ and $v[n;\theta]$ are given by (17) and (18), respectively, and where $N = n_1 - n_0 + 1$. In Appendix A, (50)–(52), respectively, give the expression of v_c, $a_{\rm ac} = V_{\rm ac}\cos(\phi_{\rm ac})$ and $b_{\rm ac} = V_{\rm ac}\sin(\phi_{\rm ac})$ as a function of $\mathbf{u}$ and $f_{\rm ac}$. Once $a_{\rm ac}$ and $b_{\rm ac}$ are estimated, the unknown acoustical parameters of θ are expressed as

$$\begin{cases} \hat{V}_{\rm ac} = \sqrt{\hat{a}_{\rm ac}^2 + \hat{b}_{\rm ac}^2} \\ \hat{\phi}_{\rm ac} = \mathrm{atan} \dfrac{\hat{b}_{\rm ac}}{\hat{a}_{\rm ac}}. \end{cases} \tag{39}$$

V. Numerical Results and Discussion

In this section, we compare the CRB with the LMS-based algorithm developed in Section IV. According to the values of the acoustic and mean flow velocities to be analyzed, the following values for $F_{\rm ac}$ and $V_{\rm ac}$ are chosen:

$$F_{\rm ac} \in [\,125 \quad 250 \quad 500 \quad 1000 \quad 2000 \quad 4000\,] \text{ Hz} \tag{40}$$

$$V_{\rm ac} \in [\,0.05 \quad 1.58 \quad 50\,] \text{ mm} \cdot \text{s}^{-1}. \tag{41}$$

$$\mathrm{var}(V_{\rm ac}) \geq \mathrm{CRB}(V_{\rm ac}) = \frac{V_{\rm ac}^2}{2\mathrm{SNR}} \frac{N^2 - \left(\frac{\sin(\gamma N)}{\sin(\gamma)}\right)^2}{\frac{N^3}{2} - \frac{N}{2}\left(\frac{\sin(2\gamma N)}{\sin(2\gamma)}\right)^2 - N\left(\frac{\sin(\gamma N)}{\sin(\gamma)}\right)^2 + \frac{\sin(2\gamma N)}{\sin(2\gamma)}\left(\frac{\sin(\gamma N)}{\sin(\gamma)}\right)^2} \tag{30}$$

$$\mathrm{var}(\phi_{\rm ac}) \geq \mathrm{CRB}(\phi_{\rm ac}) = \frac{1}{2\mathrm{SNR}} \frac{N^2 - \left(\frac{\sin(\gamma N)}{\sin(\gamma)}\right)^2}{\frac{N^3}{2} - \frac{N}{2}\left(\frac{\sin(2\gamma N)}{\sin(2\gamma)}\right)^2 - N\left(\frac{\sin(\gamma N)}{\sin(\gamma)}\right)^2 + \frac{\sin(2\gamma N)}{\sin(2\gamma)}\left(\frac{\sin(\gamma N)}{\sin(\gamma)}\right)^2} \tag{31}$$

Authorized licensed use limited to: Laurent Simon. Downloaded on July 6, 2009 at 10:10 from IEEE Xplore. Restrictions apply.

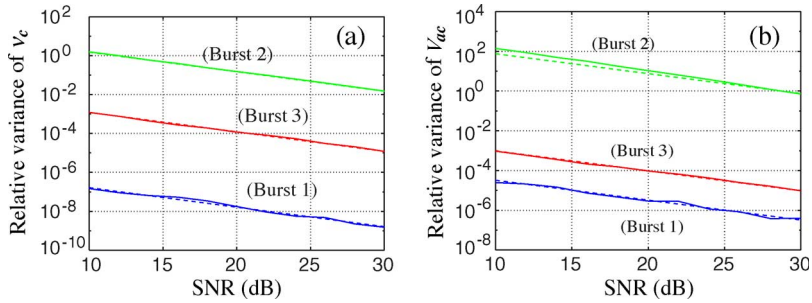

Fig. 3. Comparison of the relative variances of (a) v_c and (b) $V_{\rm ac}$ estimated by an LMS algorithm (continuous) with the theoretical CRB (dashed) for $F_{\rm ac} = 125$ Hz. Bursts (1–3) refer to Fig. 2. Burst 1: $V_{\rm ac} = 1.58$ mm $\cdot$ s^{-1}, $\alpha_v = 0.1$, and $v_c = 15.8$ mm $\cdot$ s^{-1}. Burst 2: $V_{\rm ac} = 50$ mm $\cdot$ s^{-1}, $\alpha_v = 0.1$, and $v_c = 500$ mm $\cdot$ s^{-1}. Burst 3: $V_{\rm ac} = 50$ mm $\cdot$ s^{-1}, $\alpha_v = 1$, and $v_c = 50$ mm $\cdot$ s^{-1}.

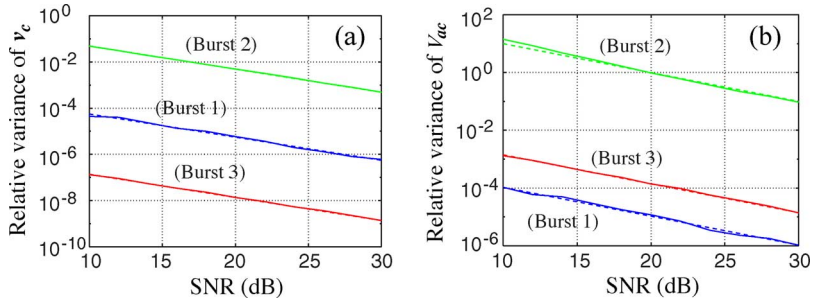

Fig. 4. Comparison of the relative variances of (a) v_c and (b) $V_{\rm ac}$ estimated by an LMS algorithm (continuous) with the theoretical CRB (dashed) for $F_{\rm ac} = 500$ Hz. Bursts (1–3) refer to Fig. 2. Burst 1: $V_{\rm ac} = 50$ mm $\cdot$ s^{-1}, $\alpha_v = 1$, and $v_c = 50$ mm $\cdot$ s^{-1}. Burst 2: $V_{\rm ac} = 50$ mm $\cdot$ s^{-1}, $\alpha_v = 0.05$, and $v_c = 1000$ mm $\cdot$ s^{-1}. Burst 3: $V_{\rm ac} = 1.58$ mm $\cdot$ s^{-1}, $\alpha_v = 0.1$, and $v_c = 15.8$ mm $\cdot$ s^{-1}.

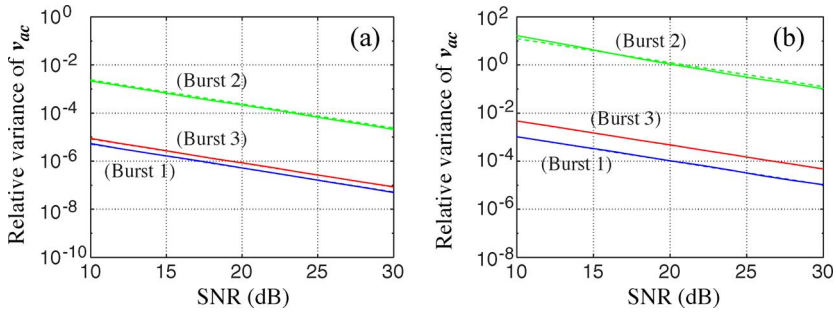

Fig. 5. Comparison of the relative variances of (a) v_c and (b) $V_{\rm ac}$ estimated by an LMS algorithm (continuous) with the theoretical CRB (dashed) for $F_{\rm ac} = 4000$ Hz. Bursts (1–3) refer to Fig. 2. Burst 1: $V_{\rm ac} = 50$ mm $\cdot$ s^{-1}, $\alpha_v = 0.1$, and $v_c = 500$ mm $\cdot$ s^{-1}. Burst 2: $V_{\rm ac} = 50$ mm $\cdot$ s^{-1}, $\alpha_v = 0.01$, and $v_c = 5000$ mm $\cdot$ s^{-1}. Burst 3: $V_{\rm ac} = 50$ mm $\cdot$ s^{-1}, $\alpha = 0.05$, and $v_c = 1000$ mm $\cdot$ s^{-1}.

The phase $\phi_{\rm ac}$ is supposed to be equal to $\pi/4$, and we use an adimensional parameter α_v for the value of v_c, such that

$$\alpha_v = \frac{V_{\rm ac}}{v_c} \in [\,0.01 \quad 0.05 \quad 0.1 \quad 0.5 \quad 1\,]. \tag{42}$$

For each numerical simulation, the sampling frequency is $F_s = 350$ kHz, the probe volume length along the x-axis is $D_x = 0.1$ mm, and 10 000 bursts are analyzed. The simulator is performed by MATLAB.

Figs. 3–5 show typical results of the relative variances (a) $\mathrm{var}(v_c)/v_c^2$ and (b) $\mathrm{var}(V_{\rm ac})/V_{\rm ac}^2$, for the different values of $F_{\rm ac}$ in comparison to the theoretical CRBs of v_c (25) and $V_{\rm ac}$ (26). Each figure is related to a given value of $F_{\rm ac}$. Furthermore, for each value of $F_{\rm ac}$, three sets of signals are analyzed, each set corresponding to one of the bursts of Fig. 2, namely $N_{\rm per} \gg 1$ (Burst 1), $N_{\rm per} > 1$ (Burst 2), and $N_{\rm per} \lesssim 1$ (Burst 3), where $N_{\rm per}$ is the number of acoustic periods $N_{\rm per} = N f_{\rm ac}$.

First, the LMS-based estimator is near the theoretical CRB, so that we can maintain that this estimator is efficient. Moreover, the relative variance of v_c is weaker than the one of $V_{\rm ac}$ (except for $\alpha_v = 1$). Indeed, for values of v_c and $V_{\rm ac}$ such that $\alpha_v = V_{\rm ac}/v_c \leq 1/\sqrt{2}$ as $\mathrm{CRB}(v_c) \simeq \mathrm{CRB}(V_{\rm ac})/2$, we have

$$\frac{\mathrm{CRB}(v_c)}{v_c^2} \leq \frac{\mathrm{CRB}(V_{\rm ac})}{V_{\rm ac}^2}. \tag{43}$$

Moreover, the values of the relative variances of v_c and $V_{\rm ac}$ drastically depend on the values of v_c, $V_{\rm ac}$, and $F_{\rm ac}$, as shown by (25) and (30).

- For $N_{\rm per} > 1$ (Burst 1), the relative variances of v_c and $V_{\rm ac}$, respectively, are in ranges of $[-70, -42]$ and

Authorized licensed use limited to: Laurent Simon. Downloaded on July 6, 2009 at 10:10 from IEEE Xplore. Restrictions apply.

TABLE I
NUMBER OF ACOUSTIC PERIODS $N_{\rm per}$ (FOR v_c AND $V_{\rm ac}$) LEADING TO AN ERROR LESS THAN E (%) FOR $F_{\rm ac} = 125$ Hz AND $V_{\rm ac} = 50$ mm $\cdot$ s^{-1}

SNR (dB)	10			20			30		
E (%)	0.1	1	10	0.1	1	10	0.1	1	10
N_{per} (v_c)	≥ 0.8	≥ 0.3	≥ 0.2	≥ 0.45	≥ 0.2	≥ 0.09	≥ 0.3	≥ 0.12	≥ 0.05
N_{per} (V_{ac})	$\gg 10$	≥ 0.75	≥ 0.25	$\gg 5$	≥ 0.5	≥ 0.2	≥ 0.8	≥ 0.25	≥ 0.1

TABLE II
NUMBER OF ACOUSTIC PERIODS $N_{\rm per}$ (FOR v_c AND $V_{\rm ac}$) LEADING TO AN ERROR LESS THAN E (%) FOR $F_{\rm ac} = 500$ Hz AND $V_{\rm ac} = 1.58$ mm $\cdot$ s^{-1}

SNR (dB)	10			20			30		
E (%)	0.1	1	10	0.1	1	10	0.1	1	10
N_{per} (v_c)	≥ 0.4	≥ 0.16	≥ 0.06	≥ 0.25	≥ 0.1	≥ 0.04	≥ 0.18	≥ 0.06	≥ 0.02
N_{per} (V_{ac})	$\gg 10$	≥ 6	≥ 0.4	$\gg 10$	≥ 0.75	≥ 0.25	$\gg 5$	≥ 0.9	≥ 0.15

TABLE III
NUMBER OF ACOUSTIC PERIODS $N_{\rm per}$ (FOR v_c AND $V_{\rm ac}$) LEADING TO AN ERROR LESS THAN E (%) FOR $F_{\rm ac} = 4000$ Hz AND $V_{\rm ac} = 50$ mm $\cdot$ s^{-1}

SNR (dB)	10			20			30		
E (%)	0.1	1	10	0.1	1	10	0.1	1	10
N_{per} (v_c)	≥ 0.6	≥ 0.25	≥ 0.1	≥ 0.4	≥ 0.15	≥ 0.05	≥ 0.25	≥ 0.1	≥ 0.03
N_{per} (V_{ac})	$\gg 20$	$\gg 5$	≥ 0.6	$\gg 10$	≥ 4.5	≥ 0.04	$\gg 10$	≥ 0.7	≥ 0.25

$[-52, -30]$ dB. Such estimations may consequently be considered as very accurate.

- For $N_{\rm per} \ll 1$ (Burst 2), the relative variances of v_c and $V_{\rm ac}$, respectively, are in ranges of $[-27, 1]$ and [10, 20] dB. The estimation of v_c is accurate enough for low values of $v_c^3 V_{\rm ac}^2 / F_{\rm ac}^4$ (32), whereas the estimation of $V_{\rm ac}$ is clearly unacceptable, regardless of the parameters v_c, $V_{\rm ac}$, and $F_{\rm ac}$ (33).
- For $N_{\rm per} \lesssim 1$ (Burst 3), the relative variances of v_c and $V_{\rm ac}$, respectively, are in ranges of $[-70, -30]$ and $[-30, -23]$ dB. Such estimations may also be considered as very accurate.

Furthermore, for velocity signals with time length largely lower than one acoustic period, we can use the asymptotic case expression of the CRBs of v_c and $V_{\rm ac}$. Giving a maximum value of the relative error, namely E_{v_c} for v_c and $E_{V_{\rm ac}}$ for $V_{\rm ac}$, we consequently have

$$\frac{\mathrm{CRB}(v_c)}{v_c^2} = \frac{1}{\mathrm{SNR}} \frac{45}{\pi^4 2^{7/2}} \frac{1}{D_x^5 F_s} \frac{v_c^3 V_{\rm ac}^2}{F_{\rm ac}^4} \leq E_{v_c} \quad (44)$$

$$\frac{\mathrm{CRB}(V_{\rm ac})}{V_{\rm ac}^2} = \frac{1}{\mathrm{SNR}} \frac{45}{\pi^4 2^{9/2}} \frac{1}{D_x F_s} \frac{v_c^5}{F_{\rm ac}^4} \leq E_{V_{\rm ac}}. \quad (45)$$

As a consequence, for a given set of setup known parameters D_x, F_s, and $F_{\rm ac}$, we may give the maximum values that $v_c^3 V_{\rm ac}^2$ and v_c^5 should have to reach to yield an error less than E_{v_c} and $E_{V_{\rm ac}}$, respectively.

Finally, from the expressions of the CRBs of v_c (25) and $V_{\rm ac}$ (30), we can calculate the number of acoustic periods that the time length of the velocity signals may have to lead to an error less than a given value E. Tables I–III give a summary of such results. Each table corresponds to a given burst of Fig. 2.

For example, Table I may be read as follows: To obtain a relative error for v_c less than 0.1% for SNR $= 10$ dB, the minimum number of acoustic periods for the velocity signal is 0.8. In the same way, to obtain a relative error for $V_{\rm ac}$ less than 1% for SNR $= 20$ dB, the minimum number of acoustic periods for the velocity signal is 0.5. Tables II and III give the minimum number of acoustic periods that the velocity signal should have to obtain relative errors less than 0.1%, 1%, and 10% for SNRs of 10, 20, and 30 dB for 500 and 4000 Hz, respectively.

As expected, the mean flow velocity v_c is estimated with a great accuracy from a very low number of acoustic periods. For example, to obtain a relative error of 1% for v_c, the number of acoustic periods is always less than 0.3, regardless of the SNR, $F_{\rm ac}$, and $V_{\rm ac}$. On the contrary, the results for the estimation of the acoustic velocity are much more contrasted. For an SNR of 30 dB, the estimation of $V_{\rm ac}$ associated with a relative error less than 1% is possible for a number of acoustic periods $N_{\rm per} > 0.9$. However, when the SNR is less than 30 dB, the number of acoustic periods associated with a relative error less than 1% may be largely bigger than 1.

The tables also show the influence of the acoustic frequency on the estimation of the particle acoustic velocity. The higher the frequency, the higher the number of acoustic periods for an accurate estimation of $V_{\rm ac}$. For a relative error of 10%, the number of acoustic periods is the same, regardless of the frequency. However, for a relative error of 1% or 0.1%, the estimation of the particle acoustic velocity is easier for a low frequency. On the contrary, the influence of the frequency on the estimation of the mean flow velocity is the opposite. The higher the frequency, the lower the number of acoustic periods for an accurate estimation.

With regard to the results of this paper, a new three-step approach can be proposed to improve the estimation of the acoustic particle velocity in the presence of mean flow. The first step consists of the estimation of the mean flow velocity for each burst with the LMS algorithm. Then, the estimation of the mean flow velocity may be subtracted from the velocity signal. Finally, a "rotating machinery" technique associated

Authorized licensed use limited to: Laurent Simon. Downloaded on July 6, 2009 at 10:10 from IEEE Xplore. Restrictions apply.

with a synchronous detection allows us to estimate the acoustic particle velocity with a great accuracy [16].

VI. Conclusion

A new method to jointly estimate the acoustic particle and the mean flow velocities from an LDV signal has been presented. It is based on the LMS algorithm and performs well in the estimation of the velocities. The performance of the method has been investigated by means of numerical tests, and the results of the simulations have been compared to the CRBs of the associated problem. It is shown that the LMS-based estimator is near the theoretical CRB so that the estimator is efficient.

Appendix A
Derivation of the LMS Problem

Inserting (18) into (38) leads to

$$V(\theta)=\frac{1}{N}\sum_{n=n_0}^{n_1}\left(u_n-\left(v_c+a_{\mathrm{ac}}\cos(2\pi f_{\mathrm{ac}}n)+b_{\mathrm{ac}}\sin(2\pi f_{\mathrm{ac}}n)\right)\right)^2 \tag{46}$$

where

$$\begin{cases} a_{\mathrm{ac}}=V_{\mathrm{ac}}\cos(\phi_{\mathrm{ac}}) \\ b_{\mathrm{ac}}=V_{\mathrm{ac}}\sin(\phi_{\mathrm{ac}}). \end{cases} \tag{47}$$

Solving the following linear problem:

$$\begin{cases} \dfrac{\partial V(\theta)}{\partial v_c}=0 \\ \dfrac{\partial V(\theta)}{\partial V_{\mathrm{ac}}}=0 \\ \dfrac{\partial V(\theta)}{\partial \phi_{\mathrm{ac}}}=0 \end{cases} \tag{48}$$

allows us to analytically write the unknown parameters. In the following, we note that

$$\begin{aligned} D=&\frac{1}{N^2}\sum_{n=n_0}^{n=n_1}\cos^2(2\pi f_{\mathrm{ac}}n)\sum_{n=n_0}^{n=n_1}\sin^2(2\pi f_{\mathrm{ac}}n) \\ &-\frac{1}{N^2}\left(\sum_{n=n_0}^{n=n_1}\cos(2\pi f_{\mathrm{ac}}n)\sin(2\pi f_{\mathrm{ac}}n)\right)^2 \\ &-\frac{1}{N^3}\sum_{n=n_0}^{n=n_1}\sin^2(2\pi f_{\mathrm{ac}}n)\left(\sum_{n=n_0}^{n=n_1}\cos(2\pi f_{\mathrm{ac}}n)\right)^2 \\ &-\frac{1}{N^3}\sum_{n=n_0}^{n=n_1}\cos^2(2\pi f_{\mathrm{ac}}n)\left(\sum_{n=n_0}^{n=n_1}\sin(2\pi f_{\mathrm{ac}}n)\right)^2 \\ &+\frac{2}{N^3}\sum_{n=n_0}^{n=n_1}\cos(2\pi f_{\mathrm{ac}}n)\sin(2\pi f_{\mathrm{ac}}n) \\ &\times\sum_{n=n_0}^{n=n_1}\cos(2\pi f_{\mathrm{ac}}n)\sum_{n=n_0}^{n=n_1}\sin(2\pi f_{\mathrm{ac}}n). \end{aligned} \tag{49}$$

The mean flow velocity v_c may then be written as

$$\begin{aligned} v_c=&\frac{1}{N^3D}\left(\sum_{n=n_0}^{n=n_1}\sin(2\pi f_{\mathrm{ac}}n)\sum_{n=n_0}^{n=n_1}\cos(2\pi f_{\mathrm{ac}}n)\sin(2\pi f_{\mathrm{ac}}n)\right. \\ &\left.-\sum_{n=n_0}^{n=n_1}\cos(2\pi f_{\mathrm{ac}}n)\sum_{n=n_0}^{n=n_1}\sin^2(2\pi f_{\mathrm{ac}}n)\right) \\ &\times\sum_{n=n_0}^{n=n_1}u_n\cos(2\pi f_{\mathrm{ac}}n) \\ &+\frac{1}{N^3D}\left(\sum_{n=n_0}^{n=n_1}\cos(2\pi f_{\mathrm{ac}}n)\sum_{n=n_0}^{n=n_1}\cos(2\pi f_{\mathrm{ac}}n)\sin(2\pi f_{\mathrm{ac}}n)\right. \\ &\left.-\sum_{n=n_0}^{n=n_1}\sin(2\pi f_{\mathrm{ac}}n)\sum_{n=n_0}^{n=n_1}\cos^2(2\pi f_{\mathrm{ac}}n)\right) \\ &\times\sum_{n=n_0}^{n=n_1}u_n\sin(2\pi f_{\mathrm{ac}}n) \\ &+\frac{1}{N^3D}\left(\sum_{n=n_0}^{n=n_1}\cos^2(2\pi f_{\mathrm{ac}}n)\sum_{n=n_0}^{n=n_1}\sin^2(2\pi f_{\mathrm{ac}}n)\right. \\ &\left.-\left(\sum_{n=n_0}^{n=n_1}\cos(2\pi f_{\mathrm{ac}}n)\sin(2\pi f_{\mathrm{ac}}n)\right)^2\right)\sum_{n=n_0}^{n=n_1}u_n. \end{aligned} \tag{50}$$

Similarly, the acoustic parameters are expressed as

$$\begin{aligned} a_{\mathrm{ac}}=&\frac{1}{N^3D}\left(\sum_{n=n_0}^{n=n_1}\sin^2(2\pi f_{\mathrm{ac}}n)\left(\sum_{n=n_0}^{n=n_1}\sin(2\pi f_{\mathrm{ac}}n)\right)^2\right) \\ &\times\sum_{n=n_0}^{n=n_1}u_n\cos(2\pi f_{\mathrm{ac}}n) \\ &+\frac{1}{N^3D}\left(\sum_{n=n_0}^{n=n_1}\cos(2\pi f_{\mathrm{ac}}n)\sum_{n=n_0}^{n=n_1}\sin(2\pi f_{\mathrm{ac}}n)\right. \\ &\left.-\sum_{n=n_0}^{n=n_1}\cos(2\pi f_{\mathrm{ac}}n)\sin(2\pi f_{\mathrm{ac}}n)\right) \\ &\times\sum_{n=n_0}^{n=n_1}u_n\sin(2\pi f_{\mathrm{ac}}n) \\ &+\frac{1}{N^3D}\left(\sum_{n=n_0}^{n=n_1}\sin(2\pi f_{\mathrm{ac}}n)\right. \\ &\times\sum_{n=n_0}^{n=n_1}\cos(2\pi f_{\mathrm{ac}}n)\sin(2\pi f_{\mathrm{ac}}n) \\ &\left.-\sum_{n=n_0}^{n=n_1}\cos(2\pi f_{\mathrm{ac}}n)\sin^2(2\pi f_{\mathrm{ac}}n)\right)\sum_{n=n_0}^{n=n_1}u_n \end{aligned} \tag{51}$$

Authorized licensed use limited to: Laurent Simon. Downloaded on July 6, 2009 at 10:10 from IEEE Xplore. Restrictions apply.

$$
\begin{aligned}
b_{\mathrm{ac}} = {} & \frac{1}{N^3 D}\left(\sum_{n=n_0}^{n=n_1}\cos^2(2\pi f_{\mathrm{ac}} n)\left(\sum_{n=n_0}^{n=n_1}\cos(2\pi f_{\mathrm{ac}} n)\right)^2\right) \\
& \times \sum_{n=n_0}^{n=n_1} u_n \sin(2\pi f_{\mathrm{ac}} n) \\
& + \frac{1}{N^3 D}\left(\sum_{n=n_0}^{n=n_1}\cos(2\pi f_{\mathrm{ac}} n)\sum_{n=n_0}^{n=n_1}\sin(2\pi f_{\mathrm{ac}} n)\right. \\
& \qquad \left. - \sum_{n=n_0}^{n=n_1}\cos(2\pi f_{\mathrm{ac}} n)\sin(2\pi f_{\mathrm{ac}} n)\right) \\
& \times \sum_{n=n_0}^{n=n_1} u_n \cos(2\pi f_{\mathrm{ac}} n) \\
& + \frac{1}{N^3 D}\left(\sum_{n=n_0}^{n=n_1}\cos(2\pi f_{\mathrm{ac}} n)\right. \\
& \qquad \times \sum_{n=n_0}^{n=n_1}\cos(2\pi f_{\mathrm{ac}} n)\sin(2\pi f_{\mathrm{ac}} n) \\
& \qquad \left. - \sum_{n=n_0}^{n=n_1}\sin(2\pi f_{\mathrm{ac}} n)\cos^2(2\pi f_{\mathrm{ac}} n)\right)\sum_{n=n_0}^{n=n_1} u_n .
\end{aligned} \tag{52}
$$

APPENDIX B
ASYMPTOTIC CRB

Here, we write the CRBs of v_c (25), V_{ac} (30), and ϕ_{ac} (31), respectively, in both asymptotic cases, i.e.,

$$2\gamma N \ll 1 \tag{53}$$

$$2\gamma N \gg 1 \tag{54}$$

where γ and $N \equiv N_q$ are given by (22) and (36), respectively. Using (36) and (22), we note that (53) and (54), respectively, are equivalent to

$$2\sqrt{2}\pi D_x F_{\mathrm{ac}} \ll v_c \tag{55}$$

$$2\sqrt{2}\pi D_x F_{\mathrm{ac}} \gg v_c. \tag{56}$$

First, we suppose that $2\gamma N \ll 1$ and that $\gamma \ll 1$, which means that the actual velocity signal corresponds to less than one acoustic period. The Taylor expansion at the seventh order of the sine functions in (25), (30), and (31), respectively, yields

$$\mathrm{var}(v_c) \geq \sigma^2 \frac{45}{\pi^4 f_{\mathrm{ac}}^4}\frac{1}{N^5} \tag{57}$$

$$\mathrm{var}(V_{\mathrm{ac}}) \geq \frac{\sigma^2}{2}\frac{45}{\pi^4 f_{\mathrm{ac}}^4}\frac{1}{N^5} \tag{58}$$

$$\mathrm{var}(\phi_{\mathrm{ac}}) \geq \frac{\sigma^2}{2V_{\mathrm{ac}}^2}\frac{45}{\pi^4 f_{\mathrm{ac}}^4}\frac{1}{N^5}. \tag{59}$$

Using (36) and (22), we note that (57)–(59), respectively, may be written as

$$\mathrm{var}(v_c) \geq \sigma^2 \frac{45}{\pi^4 2^{5/2}}\frac{1}{D_x^5 F_e}\frac{v_c^5}{F_{\mathrm{ac}}^4} \tag{60}$$

$$\mathrm{var}(V_{\mathrm{ac}}) \geq \sigma^2 \frac{45}{\pi^4 2^{7/2}}\frac{1}{D_x^5 F_e}\frac{v_c^5}{F_{\mathrm{ac}}^4} \tag{61}$$

$$\mathrm{var}(\phi_{\mathrm{ac}}) \geq \sigma^2 \frac{45}{\pi^4 2^{7/2}}\frac{1}{D_x^5 F_e}\frac{v_c^5}{F_{\mathrm{ac}}^4 V_{\mathrm{ac}}^2}. \tag{62}$$

Writing (24) into (60)–(62) leads to

$$\mathrm{var}(v_c) \geq \frac{1}{\mathrm{SNR}}\frac{45}{\pi^4 2^{7/2}}\frac{1}{D_x^5 F_e}\frac{v_c^5 V_{\mathrm{ac}}^2}{F_{\mathrm{ac}}^4} \tag{63}$$

$$\mathrm{var}(V_{\mathrm{ac}}) \geq \frac{1}{\mathrm{SNR}}\frac{45}{\pi^4 2^{9/2}}\frac{1}{D_x^5 F_e}\frac{v_c^5 V_{\mathrm{ac}}^2}{F_{\mathrm{ac}}^4} \tag{64}$$

$$\mathrm{var}(\phi_{\mathrm{ac}}) \geq \frac{1}{\mathrm{SNR}}\frac{45}{\pi^4 2^{9/2}}\frac{1}{D_x^5 F_e}\frac{v_c^5}{F_{\mathrm{ac}}^4}. \tag{65}$$

Second, we now suppose that $2\gamma N \gg 1$, which means that the actual velocity signal corresponds to greater than one acoustic period. The asymptotic CRB is then such that

$$\mathrm{var}(v_c) \geq \frac{\sigma^2}{N} \tag{66}$$

$$\mathrm{var}(V_{\mathrm{ac}}) \geq \frac{2\sigma^2}{N} \tag{67}$$

$$\mathrm{var}(\phi_{\mathrm{ac}}) \geq \frac{2\sigma^2}{N V_{\mathrm{ac}}^2}. \tag{68}$$

Using (36), we note that (66)–(68), respectively, may be written as

$$\mathrm{var}(v_c) \geq \frac{\sigma^2}{\sqrt{2}D_x F_e} v_c \tag{69}$$

$$\mathrm{var}(V_{\mathrm{ac}}) \geq \frac{\sqrt{2}\sigma^2}{D_x F_e} v_c \tag{70}$$

$$\mathrm{var}(\phi_{\mathrm{ac}}) \geq \frac{\sqrt{2}\sigma^2}{D_x F_e}\frac{v_c}{V_{\mathrm{ac}}^2}. \tag{71}$$

Finally, inserting (24) into (69)–(71) leads to

$$\mathrm{var}(v_c) \geq \frac{1}{\mathrm{SNR}}\frac{1}{2^{3/2} D_x F_e} v_c V_{\mathrm{ac}}^2 \tag{72}$$

$$\mathrm{var}(V_{\mathrm{ac}}) \geq \frac{1}{\mathrm{SNR}}\frac{1}{\sqrt{2}D_x F_e} v_c V_{\mathrm{ac}}^2 \tag{73}$$

$$\mathrm{var}(\phi_{\mathrm{ac}}) \geq \frac{1}{\mathrm{SNR}}\frac{1}{\sqrt{2}D_x F_e} v_c. \tag{74}$$

Authorized licensed use limited to: Laurent Simon. Downloaded on July 6, 2009 at 10:10 from IEEE Xplore. Restrictions apply.

REFERENCES

[1] H. E. Albrecht, N. Damaschke, M. Borys, and C. Tropea, *Laser Doppler and Phase Doppler Measurement Techniques*. New York: Springer-Verlag, 2003.

[2] W. G. P. Buchhave and J. Lumley, "The measurement of turbulence with the laser-Doppler anemometer," *Annu. Rev. Fluid Mech.*, vol. 11, pp. 443–503, 1979.

[3] L. Boyer and G. Searby, "Random sampling: Distortion and reconstruction of velocity spectra from fft analysis of the analog signal of laser Doppler processor," *J. Appl. Phys.*, vol. 60, no. 8, pp. 2699–2707, 1986.

[4] L. Simon and J. Fitzpatrick, "An improved sample-and-hold reconstruction procedure for auto-power spectra estimation of lda data," *Exp. Fluids*, vol. 37, no. 2, pp. 272–280, 2004.

[5] E. M. H. Nobach and C. Tropea, "Efficient estimation of power spectral density from laser Doppler anemometer data," *Exp. Fluids*, vol. 24, no. 5/6, pp. 499–509, 1998.

[6] R. Banning, "Spectral analysis methods for poisson sampled measurements," *IEEE Trans. Instrum. Meas.*, vol. 46, no. 4, pp. 882–887, Aug. 1997.

[7] K. Taylor, "Absolute measurement of acoustic particle velocity," *J. Acoust. Soc. Amer.*, vol. 59, no. 3, pp. 691–694, Mar. 1976.

[8] C. Greated, "Measurement of acoustic velocity fields," *Strain*, vol. 22, no. 1, pp. 21–24, 1986.

[9] K. Taylor, "Absolute calibration of microphone by laser Doppler technique," *J. Acoust. Soc. Amer.*, vol. 70, no. 4, pp. 939–945, 1981.

[10] M. Davis and K. Taylor, "Laser Doppler measurement of complex impedance," *J. Sound Vib.*, vol. 107, no. 3, pp. 451–470, 1986.

[11] J. Vignola, Y. Berthelot, and J. Jarzinsjy, "Laser detection of sound," *J. Acoust. Soc. Amer.*, vol. 90, no. 3, pp. 1275–1286, Sep. 1991.

[12] J. Sharped and C. Greated, "A stochastic model for photon correlation measurements in sound fields," *J. Phys. D, Appl. Phys.*, vol. 22, no. 10, pp. 1429–1433, Oct. 1989.

[13] J. Valière, P. Herzog, V. Valeau, and G. Tournois, "Acoustic velocity measurements in the air by means of laser Doppler velocimetry: Dynamic and frequency range limitations and signal processing improvements," *J. Sound Vib.*, vol. 229, no. 3, pp. 607–626, Jan. 2000.

[14] V. Valeau, J. Valière, and C. Mellet, "Instantaneous frequency tracking of a sinusoidally frequency-modulated signal with low modulation index: Application to laser measurements in acoustics," *Signal Process.*, vol. 84, no. 7, pp. 1147–1165, Jul. 2004.

[15] B. Gazengel and S. Poggi, "Measurement of acoustic particle velocities in enclosed sound field: Assessment of two laser Doppler velocimetry measuring systems," *Appl. Acoust.*, vol. 66, no. 1, pp. 15–44, Jan. 2005.

[16] B. Gazengel, S. Poggi, and J. Valière, "Evaluation of the performances of two acquisition and signal processing systems for measuring acoustic particle velocities in air by means of laser Doppler velocimetry," *Meas. Sci. Technol.*, vol. 14, no. 12, pp. 2047–2064, 2003.

[17] Z. Lazreq and J. Ville, "Acoustic calibration of a pressure-velocity probe," *J. Acoust. Soc. Amer.*, vol. 100, no. 1, pp. 364–371, Jul. 1996.

[18] A. Minotti, F. Simon, J. Piet, and P. Millan, "In-flow acoustic power and intensity field measurements with a 2D LDV system," presented at the AIAA/CEAS Aeroacoustic Conf., Hilton Head, SC, 2003, Paper AIAA 2003-3262.

[19] R. Boucheron, J. Valière, P. Herzog, H. Baillet, and J. Dalmont, "Evaluation of acoustic velocity in mean flow by laser Doppler velocimetry," in *Proc. 12th Int. Symp. Appl. Laser Tech. Fluid Mech.*, Lisbon, Portugal, 2004.

[20] A. Le Duff, G. Plantier, J. Valière, and R. Perdriau, "Particle detection and velocity measurements in laser Doppler velocimetry using Kalman filters," in *Proc. IEEE ICASSP*, Montréal, QC, Canada, 2004, pp. ii-365–ii-368.

[21] A. Degroot, S. Montrésor, B. Gazengel, O. Richoux, and L. Simon, "Doppler signal detection and particle time of flight estimation using wavelet transform for acoustic velocity measurement," in *Proc. IEEE ICASSP*, Toulouse, France, 2006, p. III.

[22] S. Kay, *Fundamentals of Statistical Signal Processing*, vol. I. Englewood Cliffs, NJ: Prentice-Hall, 1993.

[23] D. Rife and R. Boorstyn, "Single tone parameter estimation from discrete-time observations," *IEEE Trans. Inf. Theory*, vol. IT-20, no. 5, pp. 591–598, Sep. 1974.

[24] O. Besson and F. Galtier, "Estimating particles velocity from laser measurements: Maximum likelihood and Cramér–Rao bounds," *IEEE Trans. Signal Process.*, vol. 44, no. 12, pp. 3056–3068, Dec. 1996.

[25] W. Shu, "Cramér–Rao bound of laser Doppler anemometer," *IEEE Trans. Instrum. Meas.*, vol. 50, no. 6, pp. 1770–1772, Dec. 2001.

Laurent Simon (M'00) was born in France in 1965. He received the Ph.D. degree in acoustics from the University of Le Mans, Le Mans, France, in 1994.

He is currently a Professor with the Faculty of Science and Engineering, University of Le Mans. He is a member of the Laboratory of Acoustics, University of Le Mans (LAUM, UMR-CNRS 6613). His current research interests include time–frequency analysis methods, identification of nonlinear systems, deconvolution methods, and irregular sampling.

Olivier Richoux was born in France in 1970. He received the Ph.D. degree in acoustics from the University of Le Mans, Le Mans, France, in 1999.

He is currently a Lecturer with the Faculty of Science and Engineering, University of Le Mans. He is a member of the Laboratory of Acoustics, University of Le Mans (LAUM, UMR-CNRS 6613). His current research interests include time–frequency analysis methods, nonlinear propagation in random media, urban acoustics, and laser Doppler velocimetry for acoustics.

Anne Degroot was born in France in 1980. She is currently working toward the Ph.D. degree in acoustics with the Laboratory of Acoustics, University of Le Mans (LAUM, UMR-CNRS 6613), Le Mans, France.

Her current research interests include laser Doppler velocimetry for acoustics, timescale, and time–frequency analysis and detection.

Louis Lionet was born in France in 1978. He received the M.Sc. degree in acoustics from the University of Le Mans, Le Mans, France, in 2006.

Authorized licensed use limited to: Laurent Simon. Downloaded on July 6, 2009 at 10:10 from IEEE Xplore. Restrictions apply.